Proceedings of ICRC 2001: 1085 © Copernicus Gesellschaft 2001

ICRC 2001

Atmospheric Neutrinos in Soudan 2

M. Goodman (For the Soudan 2 Collaboration)

Argonne National Laboratory

Abstract. Neutrino interactions recorded in a 5.1 fiducial kiloton-year exposure of the Soudan-2 iron tracking calorimeter are analyzed for effects of neutrino oscillations. Using contained single track and single shower events, we update our measurement of the atmospheric ν_μ/ν_e ratio-of-ratios and find $R = 0.68 \pm 0.11 \pm 0.06$. Assuming this anomalously low R-value is the result of ν_μ flavor disappearance via ν_μ to ν_τ oscillation, we select samples of charged current events which offer good resolution, event-by-event, for L/E_ν reconstruction. Oscillation-weighted Monte Carlo events are fitted to these data events using a χ^2 function summed over bins of $\log(L/E_\nu)$. The region allowed in the $(\sin^2 2\theta, \Delta m^2)$ plane at 90% CL is obtained using the Feldman-Cousins procedure: $0.46 < \sin^2 2\theta \leq 1.0$ and $2.2 \times 10^{-4} < \Delta m^2 < 2.2 \times 10^{-2}\mathrm{eV}^2$.

1 DETECTOR; DATA EXPOSURE

The Soudan-2 experiment will soon (July 2001) be completing the taking of data using its fine-grained iron tracking calorimeter of total mass 963 tons. This detector images nonrelativistic as well as relativistic charged particles produced in atmospheric neutrino reactions. It has operated underground at a depth of 2100 meters-water-equivalent on level 27 of the Soudan Mine State Park in northern Minnesota. The calorimeter's modular design enabled data-taking to commence in April 1989 when the detector was one quarter of its full size; assembly of the detector was completed during 1993. Data-taking continued with 85% live time, even though dynamite blasting has been underway nearby for the MINOS cavern excavation since Summer 1999. The total data exposure will be $\sim$ 5.8 fiducial kiloton-years (kTy). Results presented here are based upon a 5.1 kTy exposure.

The tracking calorimeter operates as a slow-drift (0.6 cm/μs) time projection chamber. Its tracking elements are meter-long plastic drift tubes which are placed into the corrugations of steel sheets. The sheets are stacked to form a tracking lattice of honeycomb geometry. A stack is packaged as a calorimeter module and the detector is assembled building-block fashion using these modules (Allison, 1996). The calorimeter is surrounded on all sides by a cavern-liner active shield array of two or three layers of proportional tubes (Oliver, 1989).

Topologies for contained events in Soudan 2 include single track and single shower events (mostly ν_μ and ν_e quasi-elastic reactions) and multiprong events. Flavor-tagging proceeds straightforwardly: An event having a leading, non-scattering track with ionization dE/dx compatible with muon mass is a candidate charged current (CC) event of ν_μ flavor; an event having a prompt, relatively energetic shower prong is a candidate ν_e CC event. Recoil protons of momenta greater than approx. 350 MeV/c are imaged by the calorimeter, allowing a much-improved measurement of the incident neutrino direction, especially for sub-GeV quasi-elastic reactions.

2 ATMOSPHERIC ν FLAVOR RATIO

We measure the atmospheric neutrino ν_μ/ν_e flavor ratio-of-ratios R using single track and single shower events which are fully contained within the calorimeter (all hits more than 20 cm from the nearest surface). These samples contain mostly quasi-elastic neutrino reactions, but include a background of photon and neutron reactions originating in cosmic ray muon interactions in the surrounding cavern rock. The latter "rock events" are mostly tagged by coincident hits in the active shield, however some are unaccompanied by shield hits and constitute a background. The amount of zero-shield-hit rock background in a neutrino event sample is estimated by fitting event vertex-depth distributions to a combination of tagged-rock and ν Monte Carlo distributions. As expected, the fits show the background to be mostly confined to outer regions of the calorimeter. Details of our analysis procedures for quasi-elastic events can be found in (Allison, 1997) The track and shower event samples for our 5.1 kTy exposure are

Correspondence to: maury.goodman@anl.gov

summarized in Table 1. Our full detector Monte Carlo simulation of atmospheric neutrino interactions is based on the 1996 Bartol flux for the Soudan site (Agrawal 1996).

Table 1. Soudan-2 track and shower event samples from the 5.1 fiducial kiloton-year exposure.

	Tracks	Showers
Data, raw	133	193
Monte Carlo events	1097	1017
(norm. to 5.1 kTy)	193.1	179.0
Data, bkgrd subtr.	105.1±12.7	142.3±15.6

After correction for cosmic ray muon induced background, the number of single track events observed in data is less than the number of single shower events, whereas the null oscillation Monte Carlo predicts the relative rates to be otherway-round. Consequently the flavor ratio-of-ratios obtained is less than 1.0 and is anomalous:

$$R = 0.68 \pm 0.11(stat) \pm 0.06(sys).$$

3 SAMPLE FOR L/E MEASUREMENT

The phenomenology for ν_μ to ν_τ oscillations is quite specific; neutrinos of muon flavor can metamorphose and thereby "disappear" according to the equation

$$P(\nu_\mu \to \nu_\tau) = \sin^2(2\theta) \cdot \sin^2\left[\frac{1.27\,\Delta m^2[\mathrm{eV}^2] \cdot L[\mathrm{km}]}{E_\nu[\mathrm{GeV}]}\right] \quad (1)$$

Consequently it is optimal to analyze for neutrino oscillations using the variable L/E_ν. With the Soudan-2 calorimeter, measurement of event energy for charged current reactions is straightforward; we do this with resolution $\Delta E/E$ which is 20% for ν_μ CC's and 23% for ν_e CC's. To determine the neutrino path length L however, the zenith angle θ_z of the incident neutrino must be reconstructed with accuracy. The path length can be calculated from the zenith angle according to

$$L(\theta_z) = \sqrt{(R-d)^2\cos^2\theta_z + (d+h)(2R-d+h)} - (R-d)\cos\theta_z \quad (2)$$

where R is the Earth's radius, d is the depth of the detector, and h is the mean neutrino production height. The latter is a function of ν flavor, ν energy, and θ_z (Ruddick, 1998). We select from our data an event sample suited to this measurement. We use a quasi-elastic track or shower event provided that the recoil proton is measured and that P_{lept} exceeds 150 MeV/c; otherwise, if the recoil nucleon is not visible, we require the single lepton to have E_{vis} great than 600 MeV. We also select multiprong events, provided they are energetic (E_{vis} greater than 700 MeV) and have vector sum of P_{vis} exceeding 450 MeV/c (to ensure clear directionality). Additionally, the final state lepton momenta are required to exceed 250 MeV/c. For the selected sample, flavor tagging is estimated to be correct for more than 92% of events. The resolution for recovering the incident neutrino direction is evaluated using the mean angular separation between "true" versus reconstructed neutrino direction in Monte Carlo events. The mean separations are 33.2° for ν_μ CC's and 21.3° for ν_e CC's . The resolution in $\log L/E_\nu$ (L in kilometers, E_ν in GeV) is better than 0.5 for the selected sample. Hereafter we refer to these events as "HiRes events".

The zero-shield-hit rock background, as estimated by the fits to event vertex depth distributions, comprises 6.8% (5.1%) of the ν_μ (ν_e) flavor sample of HiRes events.

Table 2 shows the HiRes event populations. After background subtraction there are 106.3 data events of ν_μ flavor and 132.8 events of ν_e-flavor. Using these events, whose mean energy is higher than that of our track and shower events, the ratio-of-ratios is $R = 0.67 \pm 0.12$, which is also significantly less than 1.0.

Table 2. Event samples selected for good L/E_ν resolution, including atmospheric ν data (without, with background subtraction) and ν Monte Carlo samples. The MC rates are shown normalized to the ν_e CC data.

	ν_μ	ν_e
Data, raw	114.0±10.7	140.0±11.8
Data, subt.	106.3±14.7	132.8±13.4
Monte Carlo	158.5± 4.8	132.8±4.4

The atmospheric Monte Carlo (MC) sample represents 28.2 kiloton years of exposure. The MC event rates displayed in Table 2 have been normalized to the ν_e data sample. The assumption implicit with this adjustment is that the ν_e sample is devoid of oscillation effects. Figs. 1, and 2 show HiRes distributions with this normalization in place.

Fig. 1 shows the distributions of these samples in cosine of the zenith angle. For ν_e events, the shape of the distribution for data (Fig. 1a, crosses) coincides with that predicted by the Monte Carlo (dashed histogram) for null oscillations. The distribution of ν_μ data however, falls below the MC prediction in all bins (Fig. 1b) with the relative dearth being more pronounced for ν_μ's incident from below horizon. Distributions in $\log(L/E_\nu)$ for HiRes events are shown in Fig. 2. For null oscillations this variable distributes according to a 'phase space' which reflects the neutrino points-of-origin throughout the spherical shell volume of the Earth's atmosphere. That is, down-going ν's populate the peak at lower $\log(L/E_\nu)$ from 0.0 to 2.0. Neutrinos incident from/near the horizon occur within the dip region extending from 2.0 to 2.6, while upward-going neutrinos populate the peak at higher values. Fig. 2a shows that, allowing for statistical fluctuations, the ν_e data follows the shape of the null oscillation MC distribution. In contrast, the ν_μ data (Fig. 2b) falls below the null oscillation MC for all but the most vertically down-going flux.

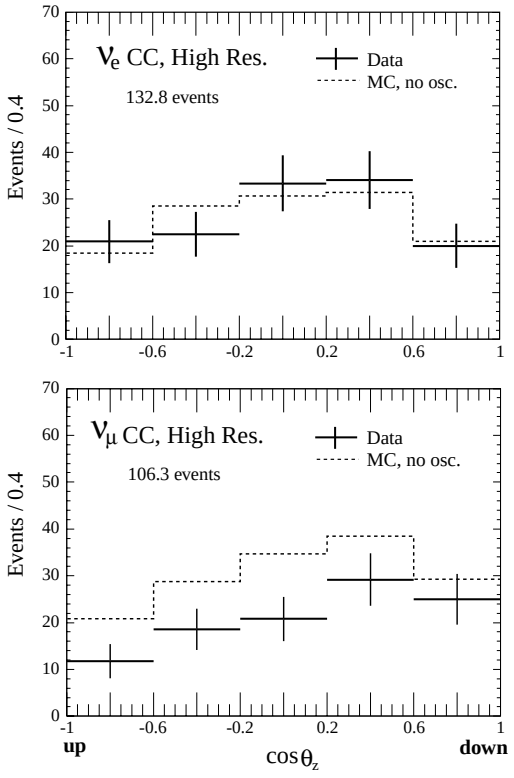

Fig. 1. Distributions of $\cos\theta_z$ for ν_e and ν_μ flavor HiRes samples. Data (crosses) are compared to the null oscillation Monte Carlo (dashed histograms) where the MC has been rate-normalized to the ν_e data.

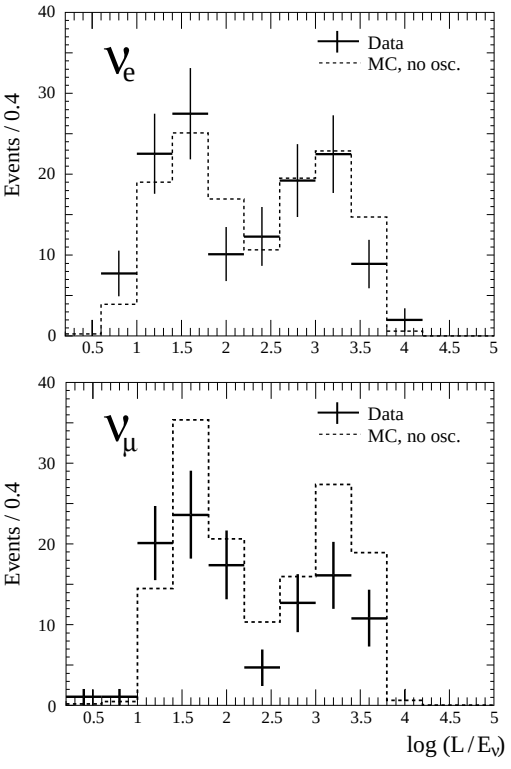

Fig. 2. Distributions of $\log(L/E_\nu)$ for ν_e and ν_μ charged current events compared to the atmospheric neutrino MC with no oscillations. The MC is shown rate-normalized to the ν_e data.

4 ($\sin^2 2\theta$, Δm^2) ALLOWED REGION

To convert results of our atmospheric neutrino simulation generated under the no-oscillation hypothesis into simulated neutrino oscillation data, we apply to every MC event an L/E_ν-dependent weight representing the probability of ν_μ flavor survival for a given Δm^2 and $\sin^2 2\theta$.

To determine the neutrino oscillation parameters Δm^2 and $\sin^2 2\theta$ from our data, we construct a χ^2 function over the plane-of-parameters. For points (i,j) in the physical region of the $(\sin^2 2\theta_i,\ \log\Delta m_j^2)$ plane, we fit the MC expectation to our data at each point. The MC flux normalization, f_ν as well as $\sin^2 2\theta_i$ and $\log\Delta m_j^2$, is a free parameter:

$$(\chi^2_{data})_{ij} = \chi^2(\sin^2 2\theta_i,\ \Delta m_j^2,\ f_\nu)$$
$$= \sum_{k=1}^{8} \frac{(N_k(data - bkgd) - f_\nu \cdot N_k(MC))^2}{\sigma_k^2}. \qquad (3)$$

We assume that the oscillation affecting our data is purely ν_μ into ν_τ and that the ν_e data is unaffected.

The χ^2 is summed over data bins containing our selected (HiRes) ν_μ and ν_e samples, where $k = 1-7$ are $\nu_\mu \log(L/E_\nu)$ bins, with $k = 8$ containing all the ν_e events. The denominator σ_k^2 accounts for finite statistics in the neutrino Monte Carlo and for uncertainty in the rock background in the ν data. Not yet included are error terms which address systematic errors in the analysis, however preliminary examination shows statistical errors to be the dominant error source in the analysis. The MC counts $N_k(MC)$ for the k^{th} bin are constructed using oscillation weight factors.

We find the location of minimum χ^2_{data}, and plot $(\Delta\chi^2_{data})_{ij}$ which is $(\chi^2_{data})_{ij} - (\chi^2_{data})_{min}$. The $\Delta\chi^2$ surface thereby obtained is shown in Fig. 3.

A crater region of low χ^2 values is clearly discerned, at the bottom of which is a relatively flat basin. The lowest point χ^2_{min} occurs at values $\sin^2 2\theta = 0.90$, $\Delta m^2 = 7.9 \times 10^{-3}$ eV^2, with flux normalization $f_\nu = 0.78$.

An additional structure is the $\Delta\chi^2$ ridge which occurs at large mixing angle and for Δm^2 above 10^{-2} eV^2 . For oscillation solutions in this regime, depletion in the downward-going ν_μ neutrino flux with sub-GeV energies is predicted for ν_μ to ν_τ oscillations by equation (1) arising from the first oscillation minimum. Our HiRes events have sufficient resolution to show such an effect if it would be present. However, no pronounced depletion is observed, and so the χ^2 has a high value there.

To find the region allowed for the oscillation parameters by our data at 90% confidence level (CL), we use the method of Feldman and Cousins (Feldman, 1998). At each of 2500 points $(i,j) = (\sin^2 2\theta_i, \Delta m_j^2)$ on a grid spanning the physical region of the plane parameters, we run 1000 simulated ex-

periments. For each of the simulated sets, we find $(\Delta\chi^2_{90})_{ij}$ such that $(\Delta\chi^2_{sim})_{ij}$ is less than $(\Delta\chi^2_{90})_{ij}$ for 90% of the simulated experiments at (i,j). The surface defined by local $\Delta\chi^2_{90}$ over the oscillation parameters plane is shown in Fig. 4. Note that the surface is not a plane at $\Delta\chi^2_{90}$ = 4.61, but rather has a concave shape. The central shaded portion is approximately $\Delta\chi^2$ = 4.6, however the outlying regions have $\Delta\chi^2$ values which are lower. At each point over the physical region, if $(\Delta\chi^2_{data})_{ij}$ is less than $(\Delta\chi^2_{90})_{ij}$, then (i,j) belongs to the allowed region of the 90% CL contour.

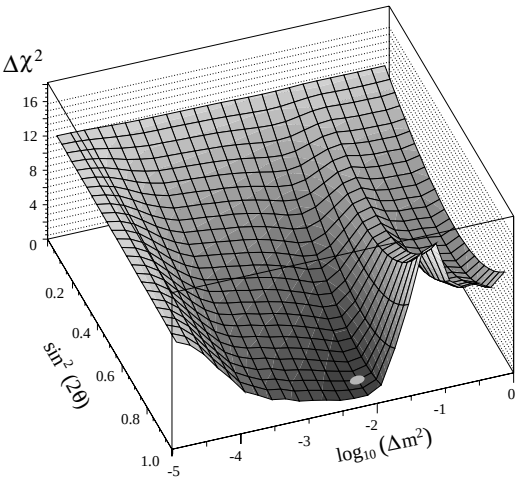

Fig. 3. The surface of $\Delta\chi^2$ over the Δm^2, $\sin^2 2\theta$ plane; the MC normalization is allowed to adjust at each point. The oval at the bottom of the basin at large mixing angle denotes the χ^2_{min} location.

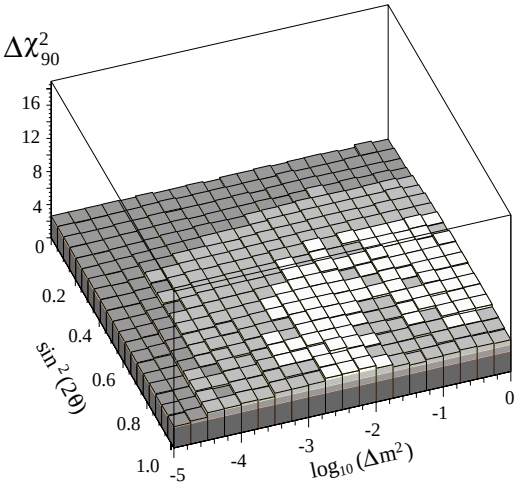

Fig. 4. The surface of $\Delta\chi^2_{90}$ over the parameters plane described via the Feldman-Cousins procedure. The intersection of this surface with the $\Delta\chi^2$ surface defines the parameters region allowed by Soudan-2 data at 90% CL.

The region allowed by our data at 90% CL is shown by the shaded area in Fig. 5. Although χ^2_{min} occurs at the location depicted by the solid circle, the relatively flat basin of our $\Delta\chi^2$ surface extends to lower Δm^2 values. SuperK has reported their best fit Δm^2 value to be 3.2×10^{-3} eV^2 (Sobel, 2000); our data is compatible with that as well as with somewhat higher Δm^2 values. We are presently updating the above analyses and expect to report new results soon.

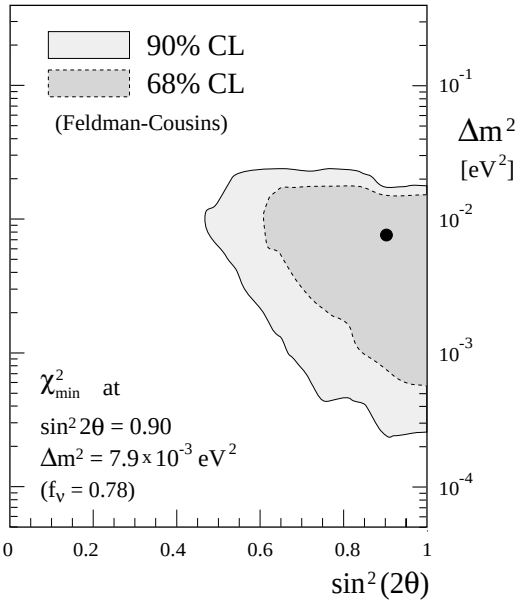

Fig. 5. Soudan-2 allowed regions at 68% and 90% CL with the best fit point for $\nu_\mu \to \nu_\tau$ oscillations.

References

W.W.M. Allison *et al.*, Nucl. Instr. Meth. **A376** (1996) 36; *ibid* **A381** (1996) 385.

W.P. Oliver *et al.*, Nucl. Instr. Meth. **A276** (1989) 371.

W.W.M. Allison *et al.*, Phys. Lett. **B 391** (1997) 491; Phys. Lett. **B 449** (1999) 137.

V. Agrawal, T.K. Gaisser, P. Lipari, and T. Stanev, Phys. Rev. **D53** (1996) 1313.

K. Ruddick, Soudan-2 internal note PDK-704 (1998), unpublished.

W.A. Mann, Plenary Talk at the XIX Int. Symposium on Lepton and Photon Interactions at High Energies, Stanford University, August 1999, hep-ex/9912007; T. Kafka, *in:* TAUP99 - Proceedings of the Sixth Int. Workshop on Topics in Astroparticle and Underground Physics, College de France, Paris, France, September 1999, Nucl. Phys. B (Proc. Suppl.) **87** (2000) 186.

G.J. Feldman and R.D. Cousins, Phys. Rev. **D 57** (1998) 3873.

H. Sobel, Proceedings of Neutrino 2000, Sudbury Canada.